Three-Surface Aircraft – Optimum vs Typical

Kamran Rokhsaz* and Bruce P. Selberg†
University of Missouri—Rolla, Rolla, Missouri

Comparisons of the induced drag for a three-surface general aviation aircraft were made using a vortex lattice method and Prandtl-Munk theory. Substantial differences between the two prediction methods have been shown in the presence of practical nonelliptic spanwise load distributions. At the same time, a parametric study using the vortex lattice method has been carried out to determine the sensitivity of lift to induced-drag ratio to different design variables. Using the resulting trends, a three-surface general aviation aircraft has been modeled and compared with its equivalent canard and conventional configurations. It has been shown that although the three-surface geometry is more efficient than a canard configuration, it remains inferior to a conventional design.

Nomenclature

$\mathcal{R}$ = aspect ratio
B = canard load/tail load
b = span
C_L = lift coefficient
C_D = drag coefficient
C_{D_i} = induced-drag coefficient
D_i = induced drag
e = efficiency factor
$\bar{G}$ = gap, vertical distance to the wing/wing span, positive above the wing
L = lift
q = dynamic pressure
$\bar{S}$ = stagger, horizontal distance to the wing/wing span
S = planform area
V = airspeed
α = geometric angle of attack
λ = taper ratio
Λ = sweep angle
σ = Prandtl's mutual induced-drag factor

Subscripts

c = canard
t = tail
w = wing

Introduction

MANY researchers have studied the effects of aerodynamic interference among the lifting surfaces on the overall efficiency of an aircraft. The simplest method of analysis was offered by Prandtl[1] for elliptically loaded surfaces. This method also takes advantage of the Munk's stagger theorem,[2] therefore being called Prandtl-Munk theory. Considering that this theory was primarily developed for hand calculations, elliptic load distribution on all surfaces plays a pivotal role in this method. Laitone[3] took advantage of this theory to demonstrate that, in the presence of a nonzero gap between the tail and the wing, the optimum induced drag can be achieved by a slight positive load on the tail. Later, he offered a modified form of the Prandtl-Munk drag formula for studying canard and tandem wing configurations in Ref. 4. By considering an elliptically loaded canard and a uniformly loaded wing, he demonstrated some differences that can arise in nonelliptic cases. Kroo[5] offered yet another modified form of the Prandtl-Munk expression for drag of a canard with elliptic load and a wing with general load distribution. These studies were all aimed at analytical solutions. McLaughlin[6] performed a comparison between the Prandtl-Munk method and vortex lattice method of determining the drag of conventional and canard configurations. Although demonstrating the efficiency of the conventional designs, he concluded that the classical theory was an accurate method for drag prediction. However, the vortex lattice method used in his study was that of Lamar,[7] which optimizes the spanwise camber and twist distributions for minimum induced drag. The drawback of this method is the resulting complex distribution of camber and twist, which may not be feasible for a general aviation aircraft.

The aforementioned studies have all been concerned with two-surface aircraft. Using the Prandtl-Munk method, Butler[8] and Kendall[9,10] studied the aerodynamic behavior of three-surface airplanes under trim conditions. Although the former showed aerodynamic gains at high lift coefficients, the latter suggested possible induced-drag reductions over the entire flight envelope in comparison with other geometries. The limited vortex lattice results presented by Rokhsaz and Selberg[11,12] and wind-tunnel tests of Ostowari and Naik[13] showed that a three-surface aircraft, while being more efficient than a canard, remains inferior to conventional designs. These studies were performed at practical static margins during cruise flight.

The purposes of this research were:

1) To compare the vortex lattice method with the Prandtl-Munk theory for canard and three-surface configurations with nonelliptic, "practical," load distributions, to determine if the Prandtl-Munk theory has any usefulness for these normal-type load distributions. Practical distributions are defined as those that would be obtained with wings having constant airfoil sections with span, constant taper, and either linear geometric twist or no twist.

2) To study the behavior of $C_{L_{trim}}/C_{D_i}$ in terms of the load ratio between the canard and the tail of three-surface aircraft.

3) Finally, to model a typical three-surface aircraft, and look at the $C_{L_{trim}}/C_{D_i}$ using the vortex lattice results in comparison with both canard and conventional configurations for various flight conditions.

Baseline Aircraft and Method of Analysis

A typical six-place business aircraft was chosen as the baseline for this study. Table 1 shows some of the characteristics of interest of the model. More detail information about weights and general geometry are given in Refs. 14 and 15. Two

Received Oct. 28, 1986; revision received Feb. 7, 1989.

*Lecturer, Mechanical and Aerospace Engineering and Engineering Mechanics. Senior Member AIAA.

†Professor, Mechanical and Aerospace Engineering and Engineering Mechanics. Associate Fellow AIAA.

additional aircraft were also formulated for the study; a canard aircraft and a three-surface aircraft. The weight and the wing area of all three aircraft were held constant. The sum of the control surface areas was also held constant between each configuration.

The lifting surfaces were analyzed with respect to inviscid flow, viscous flow, and induced drag. Viscous airfoil drag was obtained from a combination of a two-dimensional vortex panel program for the inviscid flow and a momentum integral boundary-layer method. This viscous-drag approach was taken to provide drag data for wide range of arbitrary Reynolds numbers for which published data was unavailable. The accuracty of the method has been well-documented.[14,16,17]

The induced drag was calculated using both Prandtl-Munk theory and vortex lattice method. The vortex lattice method is an expansion of Bertin and Smith[18] to take into account the effects of airfoil camber and thickness through airfoil section input data of C_{ℓ_α} and C_{ℓ_0}. The method was also extended to analyze multisurface designs. Panels of uniform width were used along the span. This method yields wing-efficiency factors, which are less than one without leaving out any of the wing span in the computation. Typical comparisons with NASA experiments are shown in Fig. 1, which has lift coefficient vs drag coefficient for an unswept wing of $\mathcal{R} = 9$. The viscous-drag component was added to the induced drag at the local C_ℓ and then integrated to get the wing C_D. The total lift coefficient was also integrated from the spanwise distribution. These predictions are very good up to when boundary-layer separation begins. This program was also expanded to estimate the longitudinal stability and control characteristics of the design and to trim the configuration by reorienting the stabilators. Figure 2 demonstrates the good accuracy of these methods when applied to the multisurface tandem wing geometry of Ref. 19.

Table 1 Six-place business aircraft

Gross take off weight	4600 lbf (approx.)
S_w	120 ft^2
$S_c + S_t$	36 ft^2
$\mathcal{R}_w$	12
$\mathcal{R}_c = \mathcal{R}_t$	9.0
$\lambda_w = \lambda_c = \lambda_t$	0.8
$C_{L_{\text{trim}}}$	0.243 (approx.)[a]
$C_{m_{o_w}}$	−0.075

[a]Corresponding to V = 500 fps at 20,000 ft

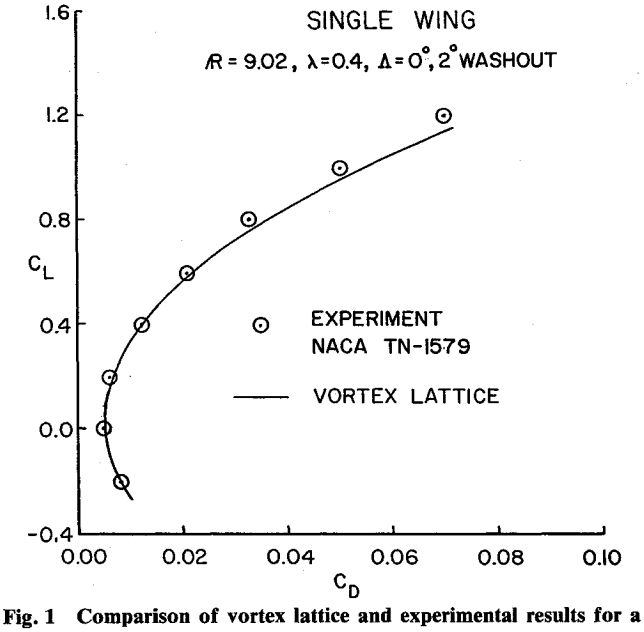

Fig. 1 Comparison of vortex lattice and experimental results for a single wing.

Longitudinal stability and trim equations used here were essentially the same as those of Refs. 11 and 12. Here again the auxiliary equation required for uniqueness in three-surface cases was taken to be

$$C_{L_c} S_c / C_{L_t} S_t = B \tag{1}$$

For the best performance, a search had to be performed for the value of B resulting in the largest value of $C_{L_{\text{trim}}}/C_{D_i}$. Static margin was set at 20% of the mean chord. This value was maintained for the generic aircraft by moving the center of gravity. For the six-place configuration, the wing was moved along with the center of gravity.

Results and Discussion

As a first step to understand the degree of error that may be introduced into the estimation of the induced drag, a canard configuration was formulated. The area of the canard was reduced in successive steps while keeping the planform characteristics the same. Parameters of interest of the canard and the wing are given in Table 2. Figure 3 shows the variation of

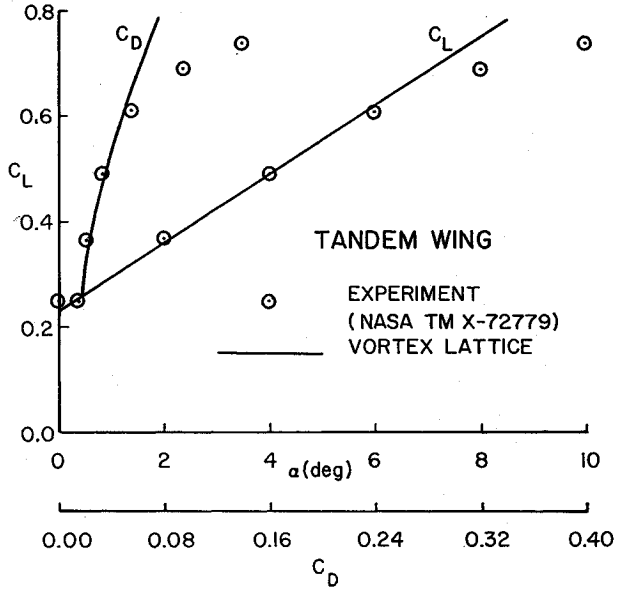

Fig. 2 Comparison of numerical and experimental results for a tandem wing configuration.

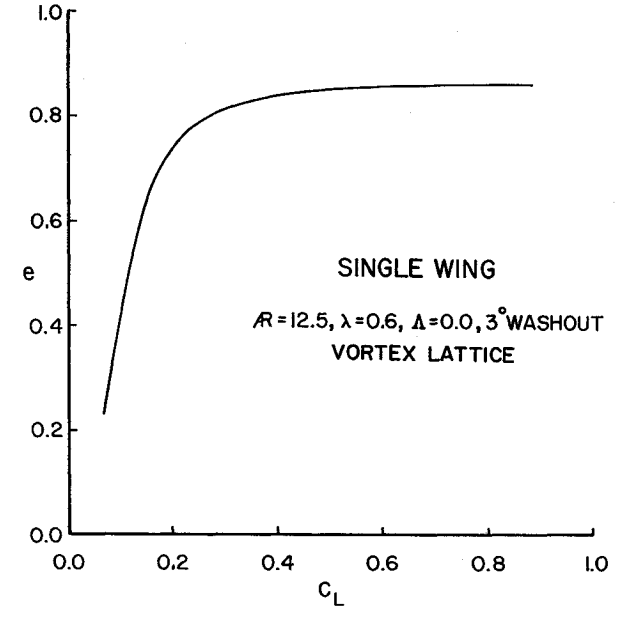

Fig. 3 Efficiency of the wing used for the canard configuration.

efficiency with lift coefficient for these planforms with 3 deg of washout. The induced drag of the coupled system was calculated using the vortex lattice model discussed earlier. The lift coefficients of both surfaces under all conditions were maintained at about 0.7, which corresponded to near-optimum efficiency of the uncoupled surfaces. With this model, trim was not of primary concern. For the total induced drag, Latione[4] gave the following relation:

$$q\pi D_i = \frac{L_w^2}{e_w b_w{}^2} + 2\left(\frac{\sigma}{e_3}\right)\frac{L_w L_c}{b_w b_c} + \frac{L_c^2}{e_c b_c{}^2} \tag{2}$$

where e_w and e_c are the efficiencies of individual surfaces when considered alone; e_3 is an additional efficiency factor associated with mutual aerodynamic interference. This expression reduces to that of the Prandtl-Munk theory if

$$e_w = e_c = e_3 = 1.0$$

Taking the induced drag calculated from the vortex lattice method, the interference parameter σ/e_3 was calculated from these expressions for two different gaps. Figures 4 and 5 show the comparison of the results with those of the Prandtl-Munk theory and Laitone's results. In both cases, the results are considerably closer to those of Laitone, even though in his cases the wing carried a uniform load. As shown in these figures, the classical Prandtl-Munk theory consistently underpredicts the total induced drag over the entire range of span ratios for gap of 0.2 and for span ratios greater than 2.0 for zero gap. Furthermore, comparison of the two figures demonstrates that aerodynamic efficiency of the total system does not improve as rapidly with increasing gap as the classical method indicates. The reason for better agreement with Laitone's method in this case is the depression of the load distribution near the midspan of the wing due to the downwash of the canard. This brings the actual variation of the load closer to a uniform distribution assumed for Laitone's method than an elliptic one as in the Prandtl-Munk theory. Results given by Kroo[5] and Lamar[7] also support this reasoning.

The next cases considered were those of the generic three-surface airplane mentioned in the previous section. The characteristics of this configuration are given in Table 3. The expression for total induced drag given by Kendall[9] is

$$q\pi D_i = \left(\frac{L_w}{b_w}\right)^2 + \left(\frac{L_c}{b_c}\right)^2 + \left(\frac{L_t}{b_t}\right)^2 + 2\sigma_{wc}\frac{L_w L_c}{b_w b_c} + 2\sigma_{wt}\frac{L_w L_t}{b_w b_t} + 2\sigma_{ct}\frac{L_c L_t}{b_c b_t} \tag{3}$$

Here, the aircraft was trimmed at static margin of 0.2. First the effects of stagger variation were considered. Figure 6 shows the ratio of trim lift to induced drag as function of the load ratio B as predicted by the Prandtl-Munk theory. Figure 7 illustrates the corresponding results from the vortex lattice method. Comparison of these figures shows that the best lift-to-induced drag ratio predicted by the classical method is considerably higher than the vortex lattice values. Also the load ratio corresponding to the highest $C_{L_{\text{trim}}}/C_{D_i}$ condition is quite far from negative unity as predicted by the Prandtl-Munk theory. Furthermore, as is evident in Fig. 7,

Table 2 Generic canard configuration

$AR_w = AR_c$	12.5
$\bar{S}_c$	0.2
$\bar{G}_c$	0.0 and 0.2
b_w/b_c	1.00 to 3.75
Washout	2 deg
$\lambda_w = \lambda_c$	0.6

Table 3 Generic three-surface configuration

$C_{L_{\text{trim}}}$	0.237
b_w	38.0 ft
$\lambda_w = \lambda_c = \lambda_t$	0.8
AR_w	12
$AR_c = AR_t$	9.8
$\bar{S}_c$	0.15, 0.25
$\bar{S}_t$	0.15, 0.25
$\bar{G}_c$	−0.2, 0.0, 0.2
$\bar{G}_t$	0.0, 0.2
$C_{m_{o_w}}$	0.10 and −0.10

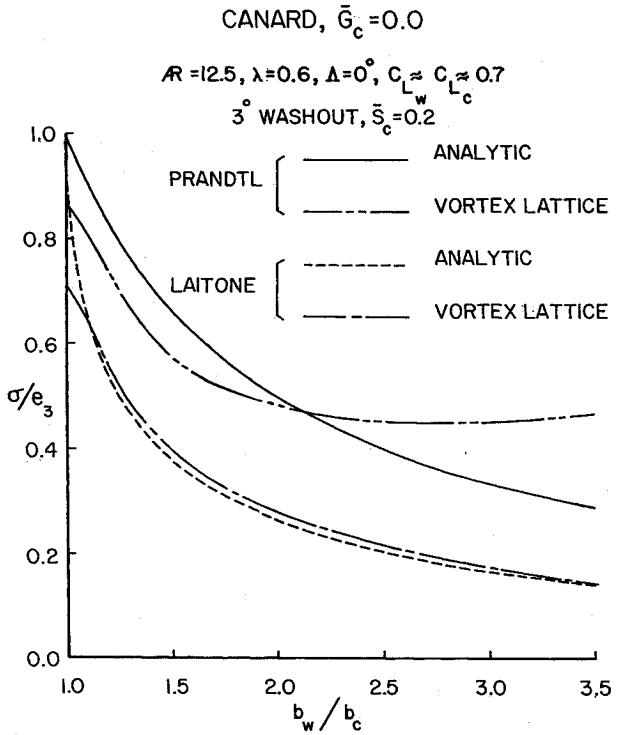

Fig. 4 Comparison of the mutual drag factors at zero gap.

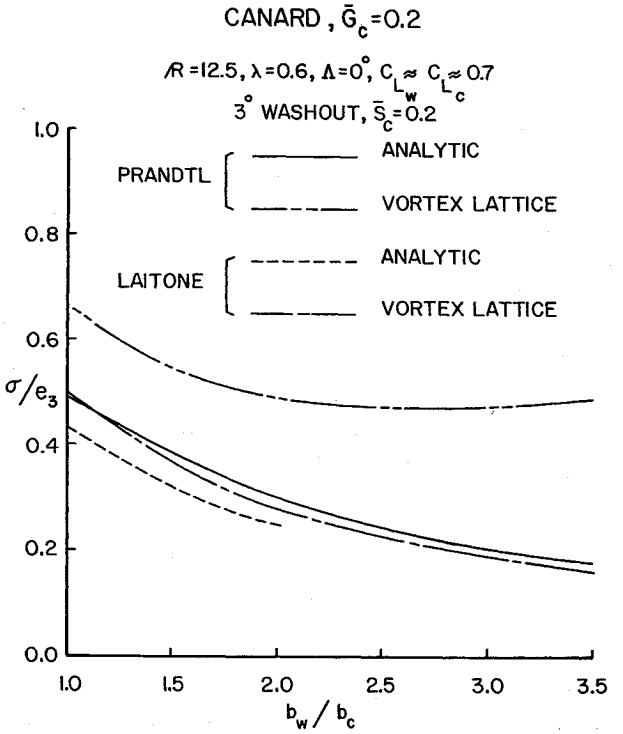

Fig. 5 Comparison of the mutual drag factors at a gap of 0.20.

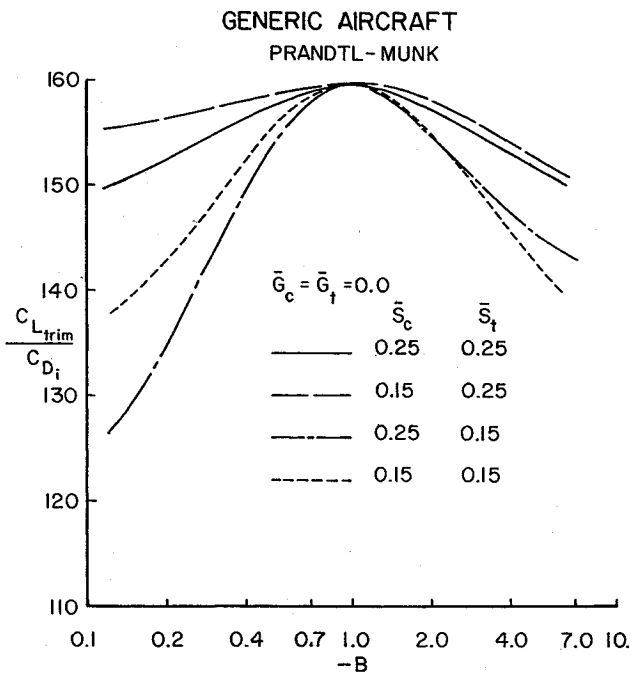

Fig. 6 Effect of stagger on $C_{L_{trim}}/C_{D_i}$ as calculated from the Prandtl-Munk formula.

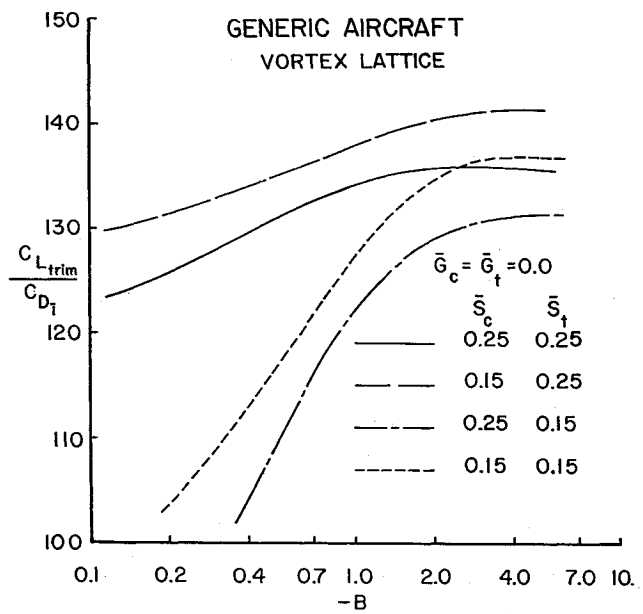

Fig. 7 Effect of stagger on $C_{L_{trim}}/C_{D_i}$ as calculated from the vortex lattice method.

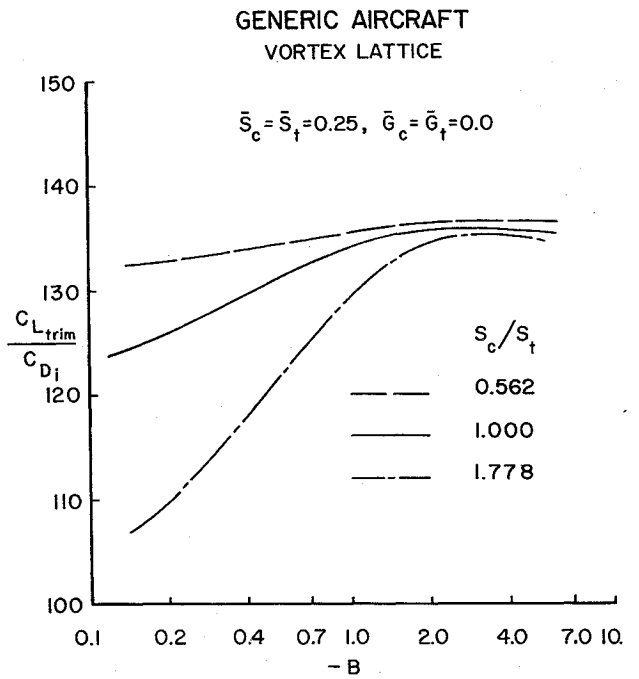

Fig. 8 Effect of the canard-to-tail-area ratio on $C_{L_{trim}}/C_{D_i}$ from vortex lattice results.

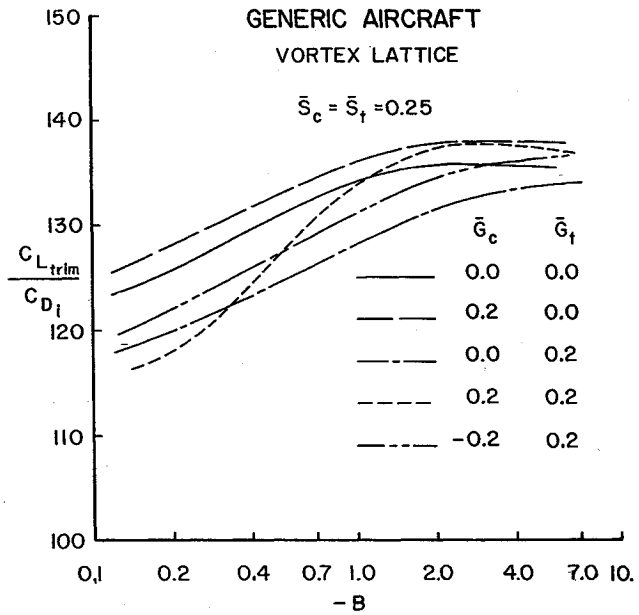

Fig. 9 Effect of gap on $C_{L_{trim}}/C_{D_i}$ from vortex lattice results.

reducing stagger of the canard increases the overall performance. From the viewpoint of stability and control, this corresponds to reducing the volume coefficient of the canard and therefore reducing its effectiveness. However, when the same reduction in the canard volume coefficient was produced by reducing its area, the maximum value of $C_{L_{trim}}/C_{D_i}$ did not increase by much. Instead, the penalty associated with off-design operation became less severe, as shown in Fig. 8. Results shown in this figure were obtained by keeping the total stabilizer area and the aspect ratio of each surface fixed.

Another parameter of interest for the three-surface case was the relative gaps. Figure 9 shows the results of varying the gaps. As shown here, the best values of lift-to-induced drag ratio are associated with positive gap of the canard. Ironically, the high-tail case appears to offer the worst performance. Also, as this figure shows, there does not appear to be a large difference among the best values of $C_{L_{trim}}/C_{D_i}$ for different configurations, but the off-design drag penalty of the high tail high canard can be rather large.

Figure 10 demonstrates the effect of the wing pithcing moment coefficient. This figure shows how the maximum value of $C_{L_{trim}}/C_{D_i}$ decreases when the wing pitching moment becomes more negative. Also, the load ratio corresponding to the best lift-to-induced-drag ratio becomes smaller in magnitude as the wing pitching moment becomes more negative. This is in contrast to Figs. 7-9, which were generated for a symmetrical wing with no pitching moment. In fact, for wing pitching-moment coefficients larger than 0.075, the load ratio became positive (i.e., upload on the tail was required for best $C_{L_{trim}}/C_{D_i}$).

Finally, the effect of trim-lift coefficient on the load ratio was studied. The value of the optimum load ratio became more negative with increasing $C_{L_{trim}}$ (from about -2.4 for a lift coefficient of 0.2 to about -16.5 for a lift coefficient of

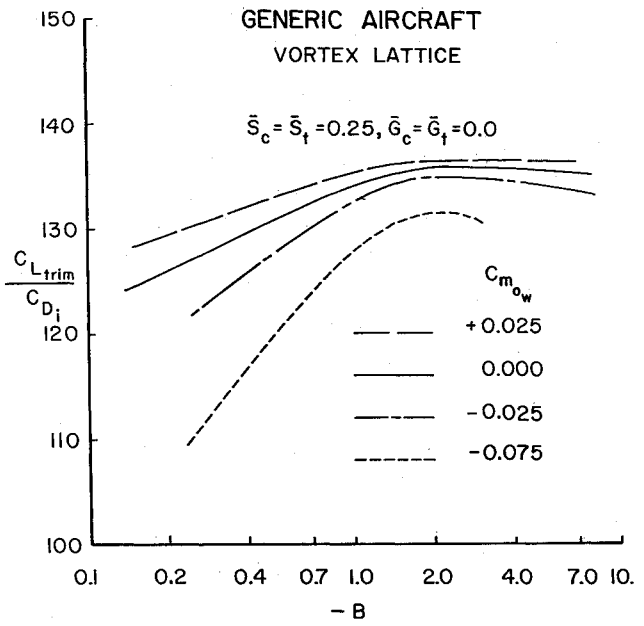

Fig. 10 Effect of wing pitching moment on $C_{L_{trim}}/C_{D_i}$ from vortex lattice results.

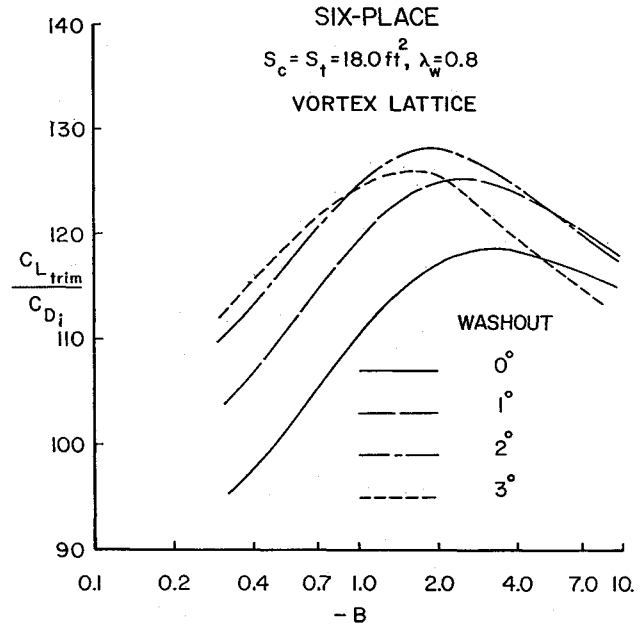

Fig. 11 Effect of wing washout on $C_{L_{trim}}/C_{D_i}$ of the six-place design from vortex lattice results.

0.8). However, $C_{L_{trim}}/C_{D_i}$ became less sensitive to the load ratio itself. At the high trim-lift coefficient of 0.8, the optimum load ratio was about -16.5 with $C_{L_{trim}}/C_{D_i}$ of 40.0. This value changed from 39.89 to 40.0 to 39.83 for load ratios of -5.25, -16.5, and $+14.7$.

Using the trends established thus far, a six-place business aircraft of advanced design was modeled. The canard and the tail areas were initially kept equal, but later the effect of area variation was also studied. Staggers of the canard and the tail were set at approximately 0.15 and 0.25, respectively. These were considered as reasonable magnitudes for a typical general aviation aircraft. These values changed slightly for the different configurations as the wing was moved to keep a fixed static margin of 0.2. The optimum gap arrangement was not attainable due to fuselage-height constraints. Since a midwing configuration was not considered feasible, all gaps were set to zero, which would simulate a top of the fuselage-mounted wing and canard with the horizontal tail mounted on the

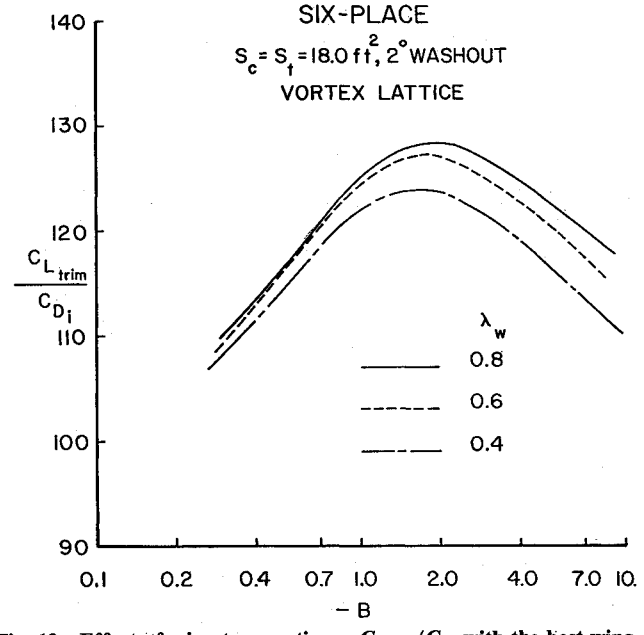

Fig. 12 Effect of wing-taper ratio on $C_{L_{trim}}/C_{D_i}$ with the best wing washout for the six-place design from vortex lattic results.

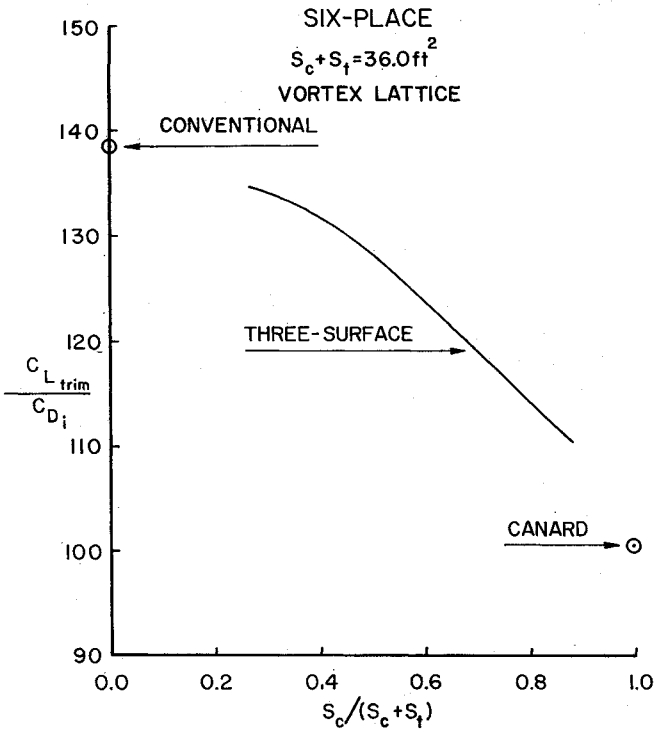

Fig. 13 Effect of area ratio on maximum $C_{L_{trim}}/C_{D_i}$ of the six-place design from vortex lattice results.

vertical stabilizer. Using vortex lattice results, Figs. 11 and 12 show the effects of the wing washout and taper on the efficiency of the configuration. As mentioned earlier, to maintain the simplicity of design, only linear twists and constant tapers were employed. In both figures, it is quite evident that the optimum load ratio approached -2.0 as the configuration became more efficient. Also, the highest lift-to-induced-drag ratio achieved in this case was 128.2. This value is in constrast with 138.4 for the conventional design and 100.5 for the canard geometry. If Prandtl-Munk theory had been applied, the best $C_{L_{trim}}/C_{D_i}$ for aircraft would be 155.0 at $B = -1.0$. The effect of changing the ratio of the canard and the tail areas on the maximum value of $C_{L_{trim}}/C_{D_i}$ is shown in Fig. 13. The design clearly became more efficient as it approached a

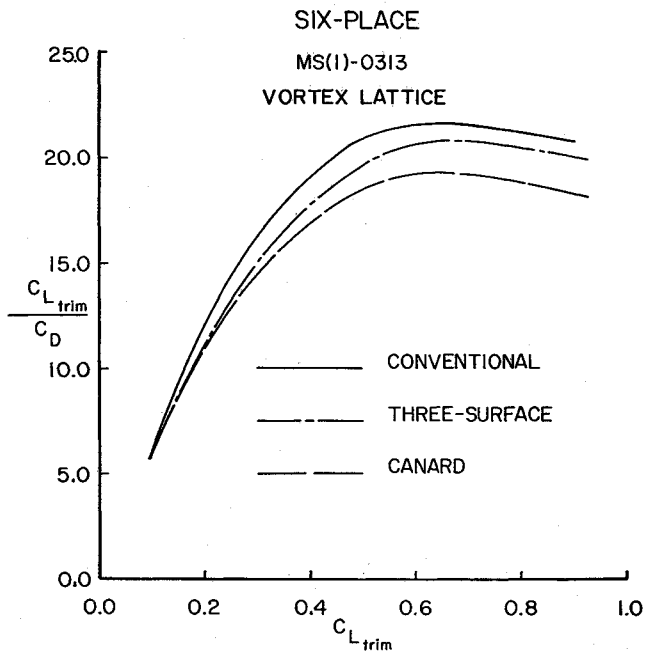

Fig. 14 Lift-to-total-drag ratio for the six-place design from vortex lattice results.

conventional geometry using the vortex lattice method. Lift-to-total drag ratio of the three configurations with viscous effects added are shown in Fig. 14. For the three-surface configuration, $S_t = S_c = 18$ ft^2, whereas for the canard and the conventional configurations, $S_c = S_t = 36$ ft^2. The wing areas for all three configurations were those that gave the best $C_{L_{trim}}/C_{D_i}$ in each respective case. All airfoils used here were the NASA MS(1)-0313. As shown in this figure, there is a very small difference among the three different geometries. However, the canard configuration with the worst $C_{L_{trim}}/C_{D_i}$ also offered the worst performance. Furthermore, the efficiency of the three-surface design did not exceed that of the conventional configuration at high lift coefficients as reported by Refs. 9 and 13. On the other hand, a close examination of the results given in Ref. 13 indicated they were obtained at close to stall lift coefficients. The linear vortex lattice method used here was not applicable in such a flight regime.

Conclusions

Comparisons were made between the Prandtl-Munk biplane theory and vortex lattice results for predicting the drag of three-surface aircraft for general aviation application. Using a generic three-surface design, the sensitivity of $C_{L_{trim}}/C_{D_i}$ to different design parameters was studied. Staggers, gaps, area ratios, wing pitching moment, and the ratio of the canard to tail loads were varied. The following points were demonstrated.

1) The Prandtl-Munk theory overpredicts the optimum $C_{L_{trim}}/C_{D_i}$ of all configurations substantially in the presence of nonelliptic spanwise load distributions. Prandtl-Munk theory also does not predict the optimum load ratio B accurately.

2) For three-surface aircraft under trim conditions, any reduction of the canard effectiveness results in improvements in the efficiency.

3) Although increasing gaps improves performance, these gains are not as large as those predicted by the classical theory.

The above findings were applied to the design of a six-place business aircraft. It was shown that the three-surface configuration, although being more efficient than a canard design, remains inferior to its equivalent conventional geometry. However, when viscous drag was included in the analysis, the differences between the three-surface and conventional geometries became very small. Considering this fact, it appears that the choice of one configuration over the other has to be made based on other factors such as structures or dynamic stability.

References

[1]Prandtl, L., "Induced Drag of Multiplanes," NASA TN-182, March 1924.

[2]Munk, M. M., "General Biplane Theory," NACA Rept 151, 1922.

[3]Laitone, E., "Positive Tail Loads for Minimum Induced Drag of Subsonic Aircraft," *Journal of Aircraft*, Vol. 15, Dec. 1978, pp. 837-842.

[4]Laitone, E., "Prandtl's Biplane Theory Applied to Canard and Tandem Aircraft," *Journal of Aircraft,* Vol. 17, April 1980, pp. 233-237.

[5]Kroo, I. M., "Minimum Induced Drag of Canard Configurations," *Journal of Aircraft*, Vol. 19, Sept. 1982, pp. 791-794.

[6]McLaughlin, M. D., "Calculations and Comparison with an Ideal Minimum of Trimmed Drag for Conventional and Canard Configurations Having Various Levels of Static Stability," NASA TN D-8391, May 1977.

[7]Lamar, J. E., "A Vortex Lattice Method for the Mean Camber Shapes of Trimmed Noncoplanar Planforms with Minimum Vortex Drag," NASA TN D-8090, June 1976.

[8]Butler, G. F., "An Analytical Study of the Induced Drag of Canard-Wing-Tail Configurations with Various Levels of Static Stability," *The Aeronautical Journal of the Royal Aeronautical Society*, Oct. 1983, pp. 293-300.

[9]Kendall, E. R., "The Theoretical Minimum Induced Drag of Three-Surface Airplanes in Trim," *Journal of Aircraft*, Vol. 22, Oct. 1985, pp. 847-854.

[10]Kendall, E. R., "The Aerodynamics of Three-Surface Airplanes," AIAA Paper 84-2508, Nov. 1984.

[11]Rokhsaz, K. and Selberg, B. P., "Analytical Study of Three-Surface Lifting Systems," Society of Automotive Engineers Paper 850866; also, *SAE Transaction,* 1986, pp. 4.554-4.564.

[12]Selberg, B. P. and Rokhsaz, K., "Aerodynamic Trade-Off Study of Conventional, Canard, and Tri-Surface Aircraft Systems," *Jouranl of Aircraft*, Vol. 23, Oct. 1986, pp. 768-774.

[13]Ostowari, C. and Naik, D. A., "Experimental Study of Three-Lifting-Surface Configuration," *Journal of Aircraft*, Vol. 25, Feb. 1988, pp. 106-112.

[14]Keith, M. W., "Parametric Canard/Wing Aerodynamic Trade-Off Analysis and Design Comparison of Canard and Conventional High-Performance General Aviation Configurations," M.S. Thesis, Univ. of Missouri, Rolla, MO, 1982.

[15]Somnay, R. J., "Design of Dual Wing Structures," M.S. Thesis, Univ. of Missouri, Rolla, MO, 1983.

[16]Rokhsaz, K., "Analytical Investigation of the Aerodynamic Characteristics of Dual Wing Systems," M.S. Thesis, Univ. of Missouri, Rolla, MO, 1980.

[17]Rhodes, M. D., and Selberg, B. P., "Benefits of Dual Wings Over Single Wings for High-Performance Business Airplanes," *Journal of Aircraft*, Vol. 21, Feb. 1984, pp. 116-127.

[18]Bertin, J. J. and Smith, M. L., *Aerodynamics for Engineers,* Prentice-Hall, Englewood Cliffs, NJ, 1979, pp. 190-195.

[19]Henderson, W. P. and Huffman, J. K., "Aerodynamic Characteristics of a Tandem Wing Configuration at a Mach Number of 0.3," NASA TM X-72779, Oct. 1975.